



Molecular cloning and functional characterization of tyrosine decarboxylases from galanthamine-producing *Lycoris radiata*

Jiawei Hu^{1,2} · Wei Li¹ · Zhan Liu^{1,2} · Guolin Zhang¹ · Yinggang Luo¹

Received: 17 June 2020 / Revised: 27 April 2021 / Accepted: 29 April 2021 / Published online: 7 May 2021
© Franciszek Górski Institute of Plant Physiology, Polish Academy of Sciences, Kraków 2021

Abstract

Tyrosine decarboxylase (TyDC), a pyridoxal-5'-phosphate (PLP)-dependent aromatic amino acid decarboxylase, catalyzes the decarboxylation of L-tyrosine (Tyr) to generate the important biogenic tyramine. This amine was reported to be a biosynthetic precursor of the Amaryllidaceae alkaloids, a group of pharmaceutically important natural products. Herein, we cloned two TyDC-encoding genes from *Lycoris radiata*, a galanthamine (GAL, a characteristic Amaryllidaceae alkaloid)-producing and medicinally and ornamentally important perennial herbaceous plant. Heterologous expression of *LrTyDCs* in *Escherichia coli* and the following purification gave recombinant *LrTyDCs* to homogeneity for enzymatic reactions. Tyramine was detected and validated by HPLC–DAD and HRESIMS analyses of the *LrTyDC*-catalyzed reaction mixture, which revealed the catalytic decarboxylation activity of *LrTyDCs*. The transcriptional *LrTyDCs* were detected in all tissues of *L. radiata* by quantitative real-time PCR analyses. The present works demonstrated that TyDC-catalyzed decarboxylation reaction is a key step to generate the non-catechol biosynthetic precursor of the Amaryllidaceae alkaloids.

Keywords Amaryllidaceae alkaloids · Biosynthesis · Tyrosine decarboxylase · *Lycoris radiata* · Galanthamine · Tyramine

Introduction

Tyramine, the decarboxylation product of L-tyrosine (Tyr) catalyzed by tyrosine decarboxylase (TyDC) (Fig. 1), is an important biogenic amine. Tyramine plays an essential role in a variety of primary physiological processes (Negrel and Javelle 2001; Kawalleck et al. 1993; Negrel et al. 1993; Trezzini et al. 1993; Borgolivier et al. 1987). Tyramine is a biosynthetic precursor of a large number of pharmaceutically important specialized metabolites such as the benzylisoquinoline alkaloids (Facchini et al. 2000, 2002) and the Amaryllidaceae alkaloids (Jin and Yao 2019; Jin 2009, 2013, 2016).

The Amaryllidaceae alkaloids (> 600 members), natural benzylphenethylamine derivatives isolated from the plants of the unique Amaryllidaceae family only, were identified with huge chemical complexities and various biological activities (Jin and Yao 2019; Jin 2009, 2013, 2016). The plants of the Amaryllidaceae family have been widely applied and ranked top 20 of the most widely applied plant families because several Amaryllidaceae alkaloids have been used in clinic (Jin 2013). Galanthamine (GAL, Fig. 1), a characteristic complex tetracyclic Amaryllidaceae alkaloid, was reported to increase acetylcholine levels via the inhibition of acetylcholinesterase and/or the allosteric modulation of nicotinic cholinergic receptor. Thus, GAL has been used to reduce the symptoms of the Alzheimer's disease patients. (Marco-Contelles et al. 2006; Marco and Carreiras 2006).

Featuring with a seven-membered azepane ring and an all-carbon quaternary stereogenic center (Fig. 1), GAL had been isolated from the plants snowdrops (*Galanthus* species), daffodils (*Narcissus pseudonarcissus*), snowflakes (*Leucojum* species), and 'red-tubed lily' and 'golden spider lily' (*Lycoris* species) (Berkov et al. 2009) of the Amaryllidaceae family. The bulbs of the aforementioned GAL-producing plants are the main tissue in which GAL is present. The contents of GAL ranged from 0.05

Communicated by P/ Wojtaszek.

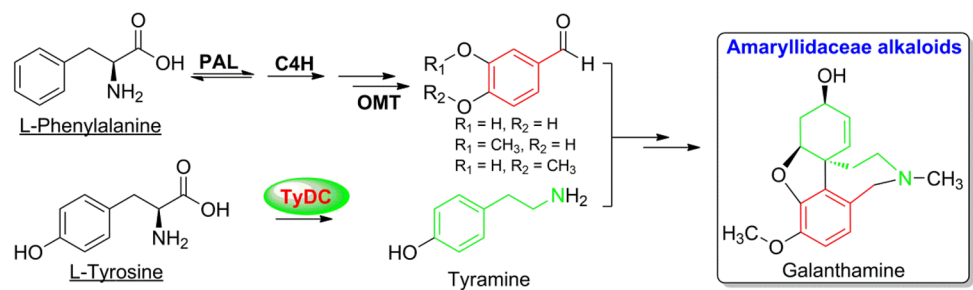
Jiawei Hu and Wei Li contributed equally to this work.

✉ Yinggang Luo
yingluo@cib.ac.cn

¹ Center for Natural Products Research, Chengdu Institute of Biology, Chinese Academy of Sciences, Chengdu 610041, People's Republic of China

² University of Chinese Academy of Sciences, Beijing 100049, People's Republic of China

Fig. 1 Biosynthetic pathway of the Amaryllidaceae alkaloids exemplified by galanthamine (GAL). PAL, phenylalanine ammonia-lyase; C4H, cinnamate 4-hydroxylase; OMT, *O*-methyltransferase; TyDC, tyrosine decarboxylase



to 0.2% (Berkov et al. 2009). The plants of the *Lycoris* genus (Amaryllidaceae family) are popular as ornamental plants (Zhou et al. 2007). Their bulbs have been used in traditional Chinese medicine to improve memory and cognitive functions (Son et al. 2010; Jin 2009). Distributed in Eastern Asian regions, *L. radiata* had been grown in China since 2002 to extract GAL (Berkov et al. 2009).

L-Phenylalanine (Phe) and L-Tyr are the two specific aromatic amino acid precursors which were integrated into the biosynthetic pathway of the Amaryllidaceae alkaloids (Fig. 1) (Barton et al. 1963). L-Phe was converted into *p*-coumaric acid via phenylalanine ammonia-lyase-catalyzed deamination of L-Phe to give *trans*-cinnamic acid and the following hydroxylation of *trans*-cinnamic acid by *trans*-cinnamate 4-hydroxylase (Fig. 1) (Desgagné-Penix 2020; Li et al. 2018; Kilgore and Kutchan 2016; Takos and Rook 2013). *p*-Coumaric acid will be oxygenated and cleaved a two-carbon unit to generate 3,4-dihydroxybenzaldehyde and its analogues that will be *O*-methylated by *O*-methyltransferase to afford the catechol moiety of the Amaryllidaceae alkaloids (Desgagné-Penix 2020; Li et al. 2019, 2018; Sun et al. 2018; Kilgore and Kutchan 2016; Kilgore et al. 2014; Takos and Rook 2013). Tyramine, the non-catechol portion of the Amaryllidaceae alkaloids, originates from L-Tyr decarboxylation reaction catalyzed by TyDC (Desgagné-Penix 2020; Sandmeier et al. 1994; Barton et al. 1963). The Mannich-like condensation reaction between the aforementioned catechol and non-catechol fragments will afford norbelladine and its analogues (Desgagné-Penix 2020; Li et al. 2019; Singh et al. 2018). The condensation products will be converted into diverse Amaryllidaceae alkaloids through oxidative phenolic coupling, rearrangement, oxidation, reduction, and *O/N*-methylation reactions (Fig. 1).

Herein, two *LrTyDCs* were cloned from GAL-producing *L. radiata* and heterologously expressed in *E. coli*. Recombinant *LrTyDCs* were shown to decarboxylate L-Tyr to form tyramine only. The transcripts of *LrTyDCs* and the content of GAL in each plant tissue were evaluated by quantitative real-time PCR and HPLC–DAD, respectively.

Materials and methods

Plant materials, total RNA isolation, and cDNA preparation

The *L. radiata* plant collection, growth, total RNA extraction and isolation, and cDNA library construction were performed, according to the reported experimental procedures (Li et al. 2018, 2019).

L. radiata transcriptome data analysis and cloning of *LrTyDCs*

Three transcriptome datasets of *L. radiata* are available in NCBI Sequence Read Archive (SRA) under the accession number SRX1597502, SRX845524, and SRX5588289, respectively. To obtain the nucleotide sequence for candidate *LrTyDC*, we mined *L. radiata* transcriptome datasets via the BLASTN analysis using the nucleotide sequences of *NpTyDC1* (GenBank accession number: KT378599) as a query for homologous alignment. Two highly homologous gene fragments, SRR1765339.26865166.1 and SRR1765339.21667464.1, were retrieved from the transcriptome data of *L. radiata* (SRX845524). The two fragments contain an overlapped region according to the multiple nucleotide sequences alignment results (Fig. S1, Supplementary Materials).

To amplify the partial fragment of candidate *LrTyDC*, a pair of gene-specific primers, *LrTyDC*-con-F and -R (Table S1, Supplementary Materials), were designed on the basis of the alignment results of the two nucleotide sequences (Fig. S1, Supplementary Materials). PCR amplification reaction was performed by using the previously prepared cDNA mixture as template and following the PCR cycling conditions: 1 cycle of 95 °C for 2 min, 35 cycles of 95 °C for 20 s, 69 °C for 20 s, and 72 °C for 4 s followed by a final extension at 72 °C for 5 min in a thermal cycler (Eppendorf AG, Hamburg, Germany). The amplified products were gel-purified and ligated into the pGM-T vector (Tiangen Biotech (Beijing) Co., Ltd.,

China). The constructs were chemically transformed into *E. coli* DH5 α competent cells and sequenced in Sangon Biotech (Shanghai) Co., Ltd. The nucleotide sequence was analyzed by using the similarity search BLAST program.

Based on the nucleotide sequence of the above confirmed amplicon of *LrTyDC*, the gene-specific primers 3'-RACE-LrTyDC-GSP1 and -GSP2 (Table S1, Supplementary Materials) were designed to perform 3'-rapid-amplification of cDNA ends (RACE) experiments. The 3'-ends of *LrTyDC* were obtained by using 3'-RACE methodology, according to the manual instructions of SMARTer™ RACE cDNA amplification kit from Clontech Laboratories. Briefly, using the previously prepared 3'-RACE-Ready cDNA as template, 3'-RACE-LrTyDC-GSP1 and Universal Primer A mix (UPM) as primers, the 3'-ends of *LrTyDC* were obtained by following the PCR cycling conditions: 1 cycle of 94 °C for 3 min; 5 cycles of 94 °C for 30 s, 72 °C for 2 min; 5 cycles of 94 °C for 30 s, 70 °C for 30 s, 72 °C for 2 min; 25 cycles of 94 °C for 30 s, 68 °C for 30 s, 72 °C for 2 min followed by a final extension at 72 °C for 10 min in a thermal cycler. The PCR products were gel-purified and used as template for the second-round PCR amplification reaction using 3'-RACE-LrTyDC-GSP2 and the Nested Universal Primer A (NUP) as primers, following the cycling conditions: 1 cycle of 94 °C for 3 min; 20 cycles of 94 °C for 30 s, 68 °C for 30 s, 72 °C for 2 min followed by a final extension at 72 °C for 10 min. The PCR products were gel-purified and ligated into the pGM-T vector. The *E. coli* DH5 α competent cells were chemically transformed with the constructs following the procedure mentioned above. The nucleotide sequences of the 3'-ends of *LrTyDC* were sequenced in Sangon Biotech Co., Ltd. Based on the nucleotide sequence of the confirmed core amplicon fragments and 3'-RACE products, the gene-specific primers 5'-RACE-LrTyDC-GSP1 and -GSP2 (Table S1, Supplementary Materials) were designed to perform 5'-RACE experiments. The 5'-ends of *LrTyDC* were obtained by using 5'-RACE methodology according to the manual instructions of SMARTer™ RACE cDNA amplification kit from Clontech Laboratories and following the identical PCR cycling conditions as described in 3'-RACE experiments. The PCR products were gel-purified and ligated into the pGM-T vector. The *E. coli* DH5 α competent cells were chemically transformed with the respective construct following the procedure mentioned above. The nucleotide sequences of the 5'-ends of *LrTyDCs* were sequenced in Sangon Biotech Co., Ltd.

LrTyDC-Full-F1, -F2, and -R (Table S1, Supplementary Materials), three gene-specific primers, were designed and synthesized to clone the full-length cDNA of *LrTyDCs*, according to the above mentioned nucleotide sequences of the core amplicon fragments, 5'- and 3'-RACE products. Using the previously prepared cDNA mixture as template and LrTyDC-Full-F1, -F2, and -R as primers, the open

reading frames (ORFs) of *LrTyDCs* were obtained by following the PCR cycling conditions: 1 cycle of 94 °C for 3 min, 35 cycles of 94 °C for 30 s, 60 °C for 30 s, and 72 °C for 2 min followed by a final extension at 72 °C for 10 min. The PCR amplified products were gel-purified, ligated into the pGM-T vector, and the resulting construct was transformed into *E. coli* DH5 α competent cells following the procedures mentioned above. The nucleotide sequences of the full length of *LrTyDCs* were sequenced and analyzed by using the similarity search BLAST program.

Bioinformatics analyses and 3-dimensional structure prediction of LrTyDCs

According to the reported procedures (Li et al. 2018, 2019), the basic bioinformatics characteristics of LrTyDCs were analyzed. The 3-dimensional structures of LrTyDCs were predicted by using the crystal of *Papaver somniferum* TyDC2 (PDB ID: 6LIU) as template. The phylogenetic tree of plant TyDCs was constructed by using the neighbour-joining method of MEGA 7.0 and the bootstrap is 1000.

Heterologous expression of LrTyDCs in *E. coli*

LrTyDC1-BH-F and -R, LrTyDC2-BH-F and -R (Table S1, Supplementary Materials) were designed and synthesized to amplify the ORFs of *LrTyDCs* from the full-length cDNA of *LrTyDCs* by using a HiFi Taq DNA polymerase (TransGen Biotech) with the following cycling conditions: 1 cycle of 94 °C for 3 min, 35 cycles of 94 °C for 30 s, 60 °C for 30 s, and 72 °C for 2 min followed by a final extension at 72 °C for 10 min. The PCR amplification products were gel-purified, digested with *Bam*H I and *Hind* III endonucleases, and ligated into the expression vector pET28a digested with the same restriction enzymes, respectively. The resulting recombinant plasmids, pET28a-LrTyDC1 and pET28a-LrTyDC2, were transformed into *E. coli* *transetta* (DE3) competent cells to generate the recombinant strains, respectively.

The expression of LrTyDCs in *E. coli* was performed according to the reported procedures (Li et al. 2019) with minor modification. Briefly, 50 μ g mL⁻¹ of kanamycin and 34 μ g mL⁻¹ of chloromycetin were supplemented into *E. coli* culture. When the optical density (OD_{600nm}) of the culture reached 0.6–0.8, 0.5 mM of isopropyl β -D-1-thiogalactopyranoside (Sangon Biotech) were added into the culture to induce the expression of the target protein. The culture was shaken at 16 °C, 160 rpm for another 19 h. The cells were harvested to separate the target enzyme by following the reported procedures (Li et al. 2019). Fractions containing His₆-tagged LrTyDCs were pooled, desalted, and concentrated by ultrafiltration using an Amicon Ultra 30 K MWCO centrifugal filter (Merck Millipore Ltd., USA) with dialysis buffer (Na₂HPO₄, 100 mM NaCl, 10% glycerol, pH

7.4, 4 °C) and stored at – 80 °C. The concentrations of LrTyDCs were estimated by using the $\epsilon_{280\text{nm}}$ 27,750 M⁻¹ cm⁻¹ (LrTyDC1) and 24,000 M⁻¹ cm⁻¹ (LrTyDC2) calculated from ExPASy ProtParam.

Enzymatic activity assay and characterization of LrTyDCs

The general enzymatic activity assays of His₆-tagged LrTyDCs were performed in 100 µL of Tris–HCl buffer (50 mM Tris, pH 8.5) containing 1 mM of PLP (purity ≥ 99%, Aladdin, China), 2 mM of L-Tyr (purity ≥ 99%, Aladdin, China), and 10 µM of enzyme. The enzyme and PLP were mixed in the buffer and incubated at 50 °C for 3 min prior to assay initiation by the addition of substrate. The reaction mixture was incubated at 50 °C with shaking at 250 rpm. An aliquot (20 µL) of the reaction mixture was sampled at 1, 3, and 48 h and quenched by adding 20 µL of chill methanol. The formation of tyramine from the enzymatic reactions was determined by HPLC–DAD equipped with an Altima C18 analytic column (250 mm × 4.6 mm, 5 µm). The mobile phase consisting of solvent A (MeOH) and solvent B (H₂O containing 0.3% trifluoroacetic acid) followed a gradient elution program (0 min, 1% solvent A; 25 min, 20% solvent A; 30 min, 99% solvent A; 31 min, 1% solvent A) at a flow rate of 1 mL min⁻¹ at 35 °C, monitored at 276 nm by a diode array detector.

L-Tryptophan (Trp), L-Phe, or 3,4-dihydroxy-L-phenylalanine (DOPA) (purity ≥ 99%, Aladdin, China) was introduced to the enzymatic activity assay system to investigate the substrate specificity of His₆-tagged LrTyDCs.

To quantitate the enzymatic tyramine from LrTyDC-catalyzed decarboxylation reactions, the reaction mixtures were directly added 1 mL of NaHCO₃-NaOH buffer (pH 10.0) and then extracted twice with ethyl acetate (2 mL × 2). After centrifugation at 10,000 rpm for 2 min, the upper layer was evaporated to dryness. The samples were re-suspended into 200 µL of NaHCO₃-NaOH buffer (pH 9.5). To the aforementioned solution the derivatization reagent dansyl chloride (DNS-Cl, dissolved in acetone, 1 eq.) was added and the resulting mixtures were incubated at 60 °C for 20 min. And then the mixtures were cooled to room temperature and the reaction was quenched by addition of 100 µL of NH₃·H₂O. The resulting mixtures were evaporated to remove acetone. The remaining mixtures were extracted twice with ether (2 mL × 2). The organic layer was evaporated to dryness after centrifugation at 10,000 rpm for 2 min. Finally, the residue was dissolved in 200 µL of methanol and the supernatant was analyzed by HPLC–DAD followed the gradient elution of solvent A (MeOH) and solvent B (H₂O) at a flow rate of 1 mL min⁻¹ and 35 °C. The gradient elution program was as follows: 0 min, 50% solvent A; 15 min, 90% solvent

A; 20 min, 100% solvent A; 26 min, 50% solvent A; monitored at 264 nm by a diode array detector.

To quantitate the formation of corresponding enzymatic products by HPLC–DAD analyses, the calibration curves of standard DNS-tyramine were established. Briefly, the same derivatization procedure was applied to prepare DNS-tyramine standard. A linear fit for the relationship of specific concentration of DNS-tyramine versus the corresponding peak area integral at 264 nm was used to plot the calibration curve.

Optimization of LrTyDC-catalyzed decarboxylation

To determine the optimal reaction temperature of LrTyDC-catalyzed decarboxylation, the reaction mixtures were incubated at 15, 20, 25, 30, 35, 40, 45, 50, 55, 60, and 70 °C. Different buffer systems were prepared as reported previously (Li et al. 2019) to determine the effects of pH value of the reaction buffer on LrTyDCs catalytic activities. The metal ions Na⁺, Fe³⁺, Fe²⁺, Mg²⁺, Zn²⁺, Mn²⁺, Ca²⁺, Cu²⁺, Li⁺, and Co²⁺ were added to the reaction solution, respectively, at a final concentration of 1 mM in the activity assay system to investigate their effects on LrTyDCs activity. All the above assays were performed in triplicate and the reaction mixtures were incubated at 50 °C, 250 rpm for 3 h.

To determine the kinetic parameters of LrTyDCs toward L-tyrosine, the reactions were performed in 100 µL of Tris–HCl buffer (50 mM Tris, pH 8.5) containing 10 µM of LrTyDCs, 1.0 mM of PLP, and L-Tyr with different concentrations (0.05–2.0 mM), respectively. All the above assays were performed in triplicate and the reaction mixtures were incubated at 50 °C, 250 rpm for 1 h. The reaction mixtures were derived with DNS-Cl as described above and the formation of DNS-tyramine was analyzed and quantitated by HPLC–DAD analyses. The steady-state kinetic constants were calculated with nonlinear regression analysis using Origin 8.0 software.

Characterization of enzymatic reaction product

To characterize the enzymatic products, a UPLC–HRESIMS was performed on a Waters Acquity I Class system equipped with an Altima C₁₈ analytic column (250 mm × 4.6 mm, 5 µm) and a Vion IMS QToF mass spectrometer. The mobile phase consisting of solvent A (MeOH) and solvent B (H₂O containing 0.1% formic acid) followed an isocratic 1% solvent A elution program for 15 min. The flow rate is 1.0 mL min⁻¹, monitored at 276 nm by a diode array detector. The injection volume of the sample was 10 µL. The electrospray ionization mass spectrometer was operated in positive ion mode and the spectra were collected in the enhanced full mass scan mode from *m/z* 50–1500.

Quantitative real-time PCR analysis of *LrTyDCs*

To quantitate the relative expression levels of *LrTyDCs* in different tissues of *L. radiata*, quantitative real-time PCR (qRT-PCR) experiments were conducted by using a CFX Connect™ real-time PCR System (Bio-Rad, USA), according to the manufacturer's instructions and previously reported procedures (Li et al. 2019). Briefly, two pairs of specific primers, rtLrTyDC1-F and -R, rtLrTyDC2-F and -R (Table S1, Supplementary Materials), were designed on the basis of the full-length cDNA sequences for real-time PCR amplification of *LrTyDCs*, according to the instructions of real-time PCR system. The relative transcriptional levels of *LrTyDCs* in different tissues were calculated by using the corresponding transcript levels of the reference gene encoding actin in the same tissue as control. The relationship between relative transcriptional levels of *LrTyDCs* and accumulation of GAL was analyzed to further determine whether LrTyDCs are involved in the Amaryllidaceae alkaloids biosynthesis in *L. radiata* (Li et al. 2019).

Results and discussion

Molecular cloning and bioinformatics properties of *LrTyDCs*

TyDCs had been cloned from plants such as *Oryza sativa* (Park et al. 2012), *Rhodiola sachalinensis* (Zhang et al. 2011), *Arabidopsis thaliana* (Lehmann and Pollmann 2009), *Rhodiola rosea* (György et al. 2009), *Aristolochia contorta* (Yang and Zeng 2005), and *Papaver somniferum* (Facchini and De Luca 1994). In view of the role of NpTyDC1 in the biosynthesis of the Amaryllidaceae alkaloids (Kilgore and Kutchan 2016), the nucleotide sequence of *NpTyDC1* (GenBank accession number: KT378599) was used as a query to mine the public available transcriptome datasets of *L. radiata* from NCBI SRA. A candidate *LrTyDC* fragment was assembled on the basis of the multiple nucleotide sequences alignment results (Fig. S1, Supplementary Materials). Based on a homology cloning strategy, a 171-bp gene fragment of *LrTyDC* was obtained from a PCR amplification reaction. Subsequent 3'- and 5'-RACE experiments afforded the 3'- and 5'-end fragments, respectively. The full-length cDNA sequence of *LrTyDCs* was generated by overlapping the aforementioned DNA fragments, which was confirmed by the following full-length PCR amplification reactions and subsequent DNA sequencing. Two DNA sequences were obtained. One is 1536-bp which encodes a protein with 511 amino acid residues and it was designated as LrTyDC1 (GenBank accession number: MT468182). LrTyDC2 (GenBank accession number: MT468183) was shown to have 510 amino acid residues that is encoded by a 1533-bp ORF.

It should be noted that a *TyDC* from *L. radiata* was deposited in NCBI on October 22, 2019 with GenBank accession number: MK690193. Multiple amino acid residue sequence alignment analyses showed that a serine highlighted by the blue arrow is present in all functionally characterized plant *TyDCs* (Fig. 2). Previous studies revealed that mutation of Ser372 of PsTyDC into Gly enables the mutant PsTyDC to use 5-hydroxytryptophan as a substrate and reduces the enzyme activity toward L-DOPA (Torrens-Spence et al. 2014). However, the reverse mutation in a *Catharanthus roseus* tryptophan decarboxylase (CrTDC) enabled the mutant enzyme to utilize L-Tyr and L-DOPA substrates with a reduced affinity toward L-Trp (Torrens-Spence et al. 2014). Both *TyDC* and *TDC* are plant aromatic amino acid decarboxylase but they exhibit different substrate specificity (Facchini and De Luca 1995). It is a Gly in the corresponding site in the partial CDS of the previously deposited *LrTyDC*, we propose that it might be a *TDC* rather than a *TyDC* in *L. radiata*.

By using the ExpASY online tools, the theoretical isoelectric point and the molecular weight of LrTyDC1 were predicted to be 4.93 and 62.84 kDa, respectively, while for LrTyDC2, they are 4.93 and 62.93 kDa. LrTyDCs shares 47.9–97.3% amino acid residue identities and similarities with the functionally characterized plant *TyDCs* (Fig. 2 and Fig. S2, Supplementary Materials). LrTyDCs were shown to contain the following characteristic features of plant *TyDCs* (Fig. 2) (Wang et al. 2020). The highly conserved catalytic amino acid K321 in LrTyDC1 (K319 in LrTyDC2) covalently binds to PLP to form an internal aldimine. The key active sites (D289, N318, and S372 in LrTyDC1; and D287, N316, and S370 in LrTyDC2) coordinate with PLP via hydrogen bonds. The highly conserved amino acid residues F126, H205, and T264 in LrTyDC1 (F124, H203, and T263 in LrTyDC2) involve in binding and stabilizing cofactor PLP. The conserved loop (WQIALSRRFR) involves in interactions with phosphate group of PLP to anchor PLP. The phylogenetic tree analysis revealed that LrTyDC1 and LrTyDC2 are phylogenetically close to the functionally characterized NpTyDC1 (Singh and Desgagné-Penix 2017; Kilgore and Kutchan 2016) and LaTyDC1 (Wang et al. 2019). The afore-mentioned information implied that LrTyDCs might function in GAL's biosynthetic pathway (Fig. 3). The 3-dimensional structure of LrTyDCs (Fig. 4) was predicted by using the SWISS-MODEL online software (<http://www.swissmodel.expasy.org>) in which the crystal structure of PsTyDC2 (PDB ID: 6LIU, Wang et al. 2020) from *Papaver somniferum* that shares 73.56% and 74.21% amino acid residue identities with LrTyDC1 and LrTyDC2, respectively, was identified to be a template. Predicted models showed that LrTyDC1 and LrTyDC2 are homodimeric structures (Fig. 4a and c) and each monomer consists of catalytic amino acid residues and conserved domains (Fig. 4b and d).

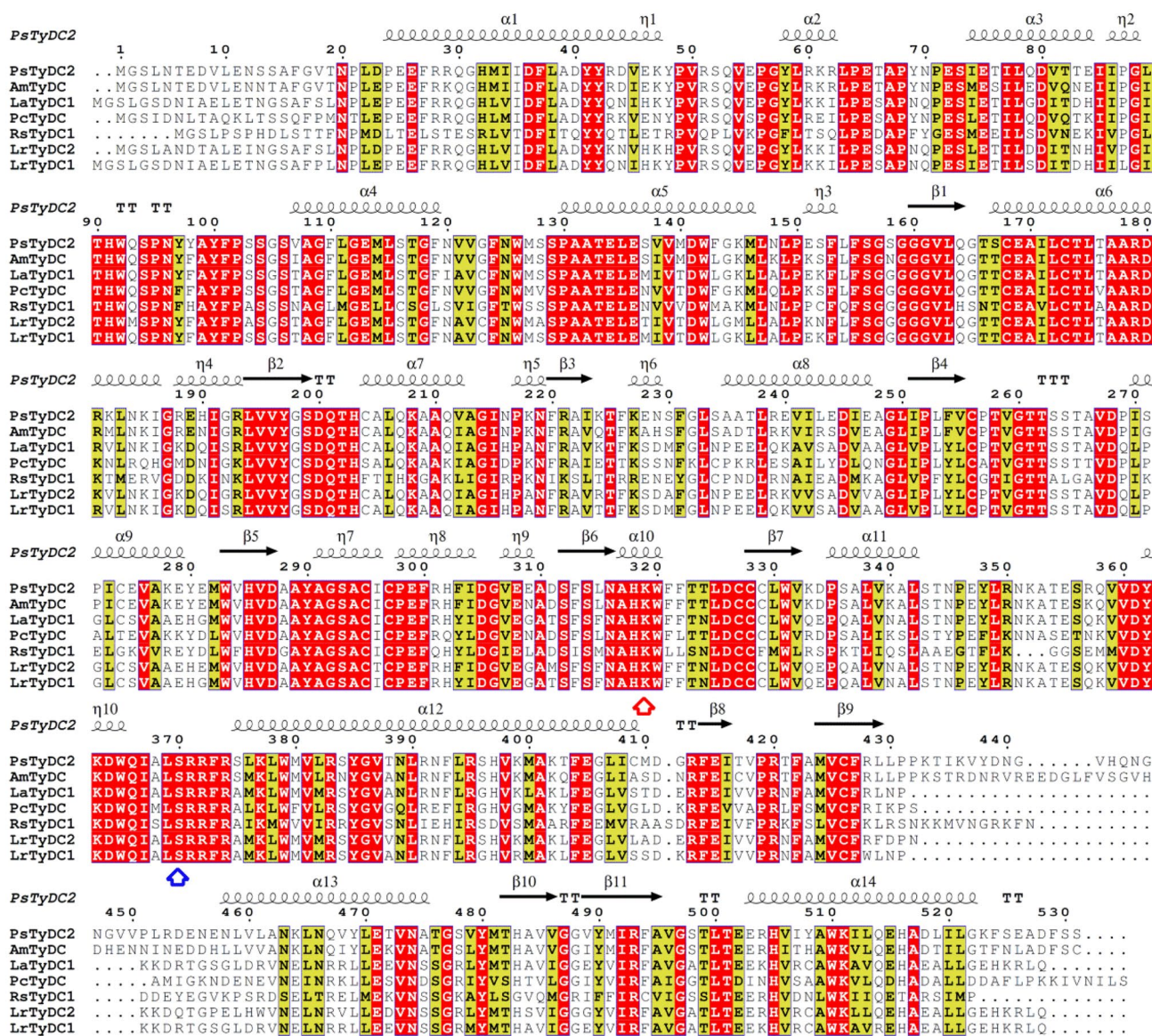


Fig. 2 Multiple amino acid residue sequences alignment of LrTyDCs and the functionally characterized plant TyDCs by using online Clustal Omega multiple alignment tool. The results were graphed by using ESPrnt 3.0 software. The crystal structure of PsTyDC2 (PDB ID: 6LIU, P54769.1) was used as model. AmTyDC, ACJ76782.1; LaTyDC1, AYH64864.1; PcTyDC, AAA33861.1; RsTyDC1,

ABF06560.1. The highly conserved amino acid residues were highlighted in red and the secondary highly conserved amino acid residues were highlighted in yellow. The catalysis lysine (K) was indicated by a vertical red arrow and the key serine (S) was indicated by a vertical blue arrow

Heterologous expression and catalytic function of LrTyDCs

The two *LrTyDCs* were heterologously overexpressed in *E. coli transetta* (DE3) cells via pET28a expression vector. The homogeneous N-terminal His₆-tagged recombinant LrTyDCs were obtained via affinity column chromatography (Fig. S3, Supplementary Materials). The LrTyDC-catalyzed decarboxylation activity assays were carried out by incubation of L-Tyr, PLP, and LrTyDCs or boiled LrTyDCs.

A new peak was observed in LrTyDC-catalyzed reaction mixture that was analyzed by HPLC–DAD (panels II and IV, Fig. 5a), compared with the control reactions in which the boiled LrTyDCs were used as catalysts (panels III and V, Fig. 5a). The aforementioned peaks have identical retention time to that of the standard tyramine (panel I, Fig. 5a). The two products showed identical protonated ion at *m/z* 138.05496 [M + H]⁺ in the HRESIMS analyses (Fig. S4, Supplementary Materials), which is in perfect conformity with that of authentic tyramine. Thus both LrTyDCs

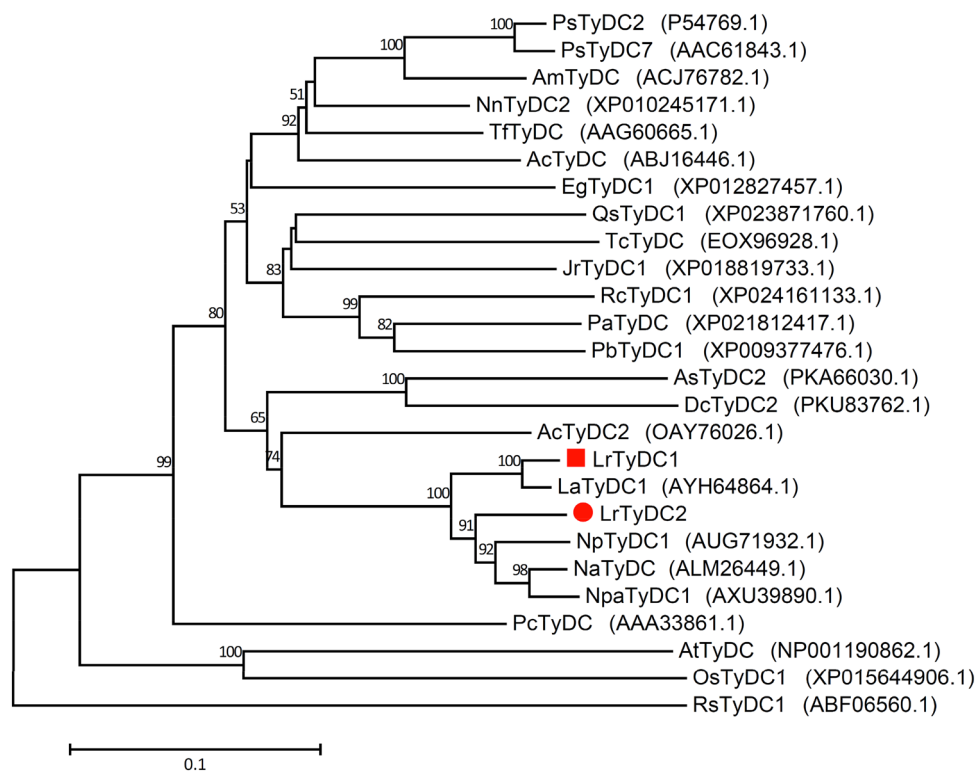


Fig. 3 Phylogenetic tree of plant TyDCs. The amino acid residue sequences were retrieved from the National Center for Biotechnology Information database (<http://www.ncbi.nlm.nih.gov/>). Phylogenetic analysis was performed by using the MEGA 7.0 software package and neighbor-joining program (<http://www.megasoftware.net/>). The computation was performed with 1000 bootstrap replicate and a Poisson correction. The bootstrap values higher than 50% are given at the nodes. The scale bar indicates the phylogenetic distance calculated from the number of differences. LrTyDC1 from *Lycoris aurea*; NpTyDC1 from *Narcissus pseudonarcissus*; NaTyDC *Narcissus aff. pseudonarcissus* MK-2014; NpaTyDC1 from *Narcissus papyra-*

ceus; EgTyDC1 from *Erythranthe guttata*; NnTyDC2 from *Nelumbo nucifera*; DcTyDC2 from *Dendrobium catenatum*; QsTyDC1 from *Quercus suber*; AcTyDC from *Aristolochia contorta*; TfTyDC from *Thalictrum flavum subsp. Glaucum*; OsTyDC1 from *Oryza sativa* Japonica Group; RsTyDC1 from *Rhodiola sachalinensis*; AcTyDC2 from *Ananas comosus*; AsTyDC2 from *Apostasia shenzhenica*; RcTyDC1 from *Rosa chinensis*; JrTyDC1 from *Juglans regia*; PbTyDC1 from *Pyrus bretschneideri*; PcTyDC from *Petroselinum crispum*; PaTyDC from *Prunus avium*; PsTyDC2 and PsTyDC7 from *Papaver somniferum*; AmTyDC from *Argemone mexicana*; AtTyDC from *Arabidopsis thaliana*; TcTyDC from *Theobroma cacao*

exhibited decarboxylation activity and LrTyDC1 showed higher activity than LrTyDC2 (panels II and IV, Fig. 5a).

However, the decarboxylated product of the LrTyDC1-catalyzed decarboxylation reaction (48 h) showed ~ 10 mAU absorption at 276 nm, the characteristic maximum wavelength in the HPLC–DAD condition used in the present work (panel II, Fig. 5a). To enhance the sensitivity of the HPLC–DAD analyses and quantitate the products, the enzymatic products and standard tyramine were separately derived with DNS-Cl (Wu et al. 2018; Zhang et al. 2018). DNS-tyramine showed a sharp peak (panel I, Fig. 5b) in the HPLC–DAD condition used in the present work. DNS-tyramine with ~ 30 mAU absorption at the characteristic maximum wavelength of 264 nm was observed when the LrTyDC1-catalyzed decarboxylation reaction was performed for 3 h (panel II, Fig. 5b).

The optimal enzymatic reaction conditions for LrTyDC-catalyzed decarboxylation are 50 °C (Fig. S5A and 5D,

Supplementary Materials) and pH 8.5 (Fig. S5B and 5E, Supplementary Materials) under which LrTyDCs exhibit the maximum catalytic activity. The decarboxylation activity of LrTyDCs was displayed with a slight change when the enzymatic reaction was performed with the addition of different metal ions (Fig. S5C and 5F, Supplementary Materials). The enzymatic activity of LrTyDCs was inhibited by the addition of Fe^{2+} , Fe^{3+} , and Li^+ (Fig. S5C and 5F, Supplementary Materials). The metal ions Na^+ , Zn^{2+} , Mg^{2+} , Mn^{2+} , Ca^{2+} , and Co^{2+} were shown to slightly increase the decarboxylation activity of LrTyDCs (Fig. S5C and 5F, Supplementary Materials). The apparent kinetic parameters K_m and V_{max} for LrTyDC1-catalyzed decarboxylation reaction are 0.39 ± 0.14 mM and 3.15 ± 0.84 $\mu\text{M min}^{-1}$, respectively (Fig. 6). LrTyDC1 showed similar K_m and V_{max} to LaTyDC1 (Wang et al. 2019), which is consistent with the phylogenetic tree analyses (Fig. 3). LrTyDC2 showed higher affinity and lower reaction rate and the K_m and V_{max}

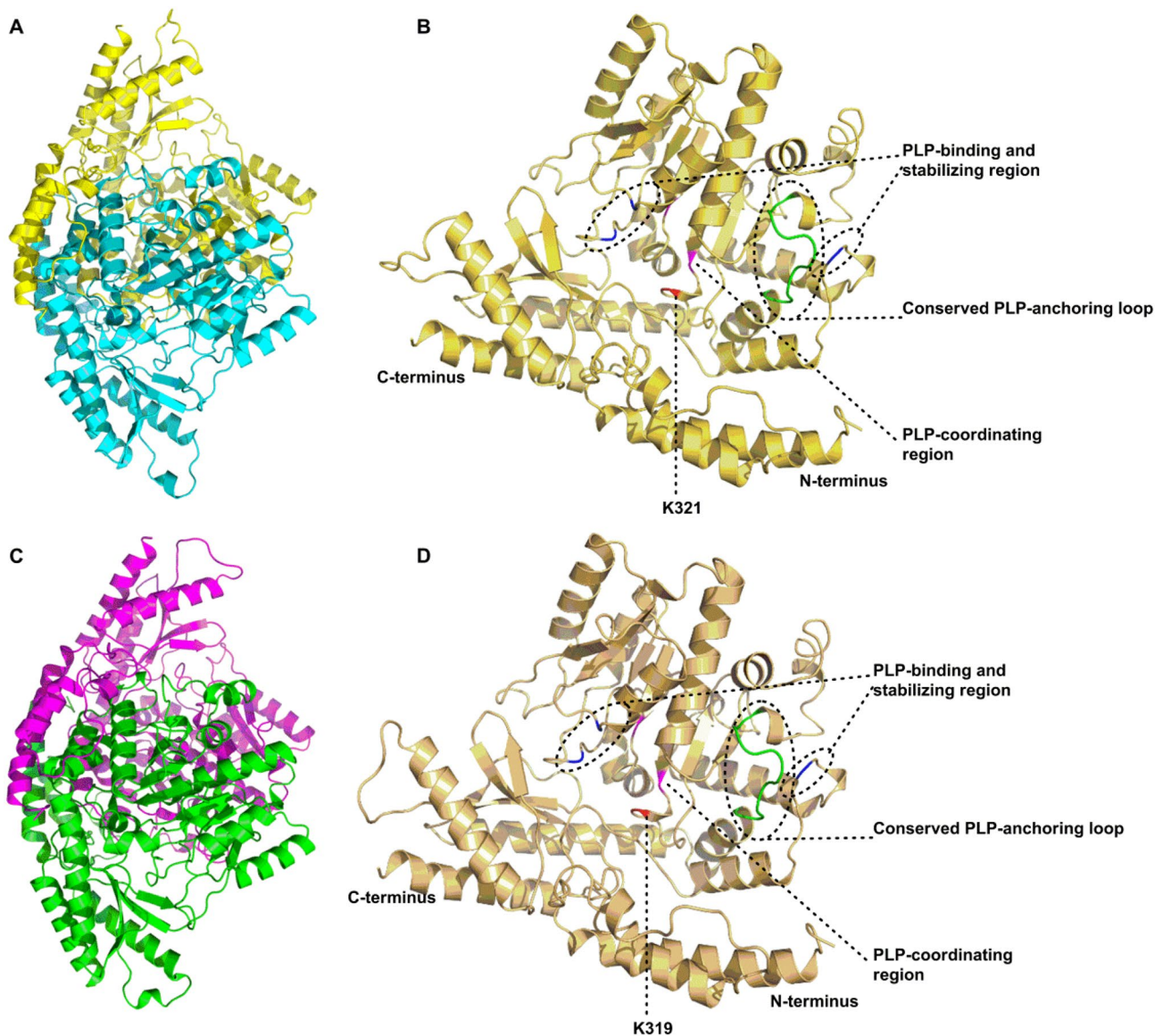


Fig. 4 The predicted 3-D structure of LrTyDCs. Ribbon diagram of quaternary structure of LrTyDC1 (a) and LrTyDC2 (c) homodimer. Schematic key active regions of the monomer of LrTyDC1 (b) and LrTyDC2 (d). The crystal structure of *Papaver somniferum* TyDC2 (PDB ID: 6LIU) was used as model template to construct the

3-dimensional structure of LrTyDCs. The PLP-binding, -stabilizing, -anchoring, and -coordinating regions were indicated. The catalytic lysine was illustrated. The graphic was generated by PyMOL molecular visualization system

values for LrTyDC2-catalyzed decarboxylation reaction are 0.06 ± 0.007 mM and 2.64 ± 0.04 $\mu\text{M min}^{-1}$, respectively (Fig. 6).

Animal TyDCs can recognize and catalyze the decarboxylation of L-Tyr and its analogues, including L-DOPA, L-Trp, L-Phe, and L-His, to generate the corresponding decarboxylated products (Christenson et al. 1972). Nevertheless, plant TyDCs usually show high substrate specificity (Marques and Brodelius 1988; Noé et al. 1984; Christenson et al. 1972). L-Tyr was the native substrate of the TyDC from *Rhodiola sachalinensis* involved in the biosynthesis

of salidroside (Zhang et al. 2011). L-DOPA and L-Phe could be decarboxylated by *Rhodiola sachalinensis* TyDC but L-Trp could not be accepted by the aforementioned TyDC (Zhang et al. 2011). *Arabidopsis thaliana* TyDC recognized L-Tyr only (Lehmann and Pollmann 2009). *Papaver somniferum* TyDC5 showed decarboxylation activity toward L-Tyr, L-DOPA, and L-Phe (Maldonado-Mendoza et al. 1996). No activity was observed when L-Trp was used as substrate of PsTyDC5 (Maldonado-Mendoza et al. 1996). PsTyDC1 and PsTyDC2 could accept L-Tyr and L-DOPA (Facchini and De Luca 1994). L-Trp and L-Phe were not

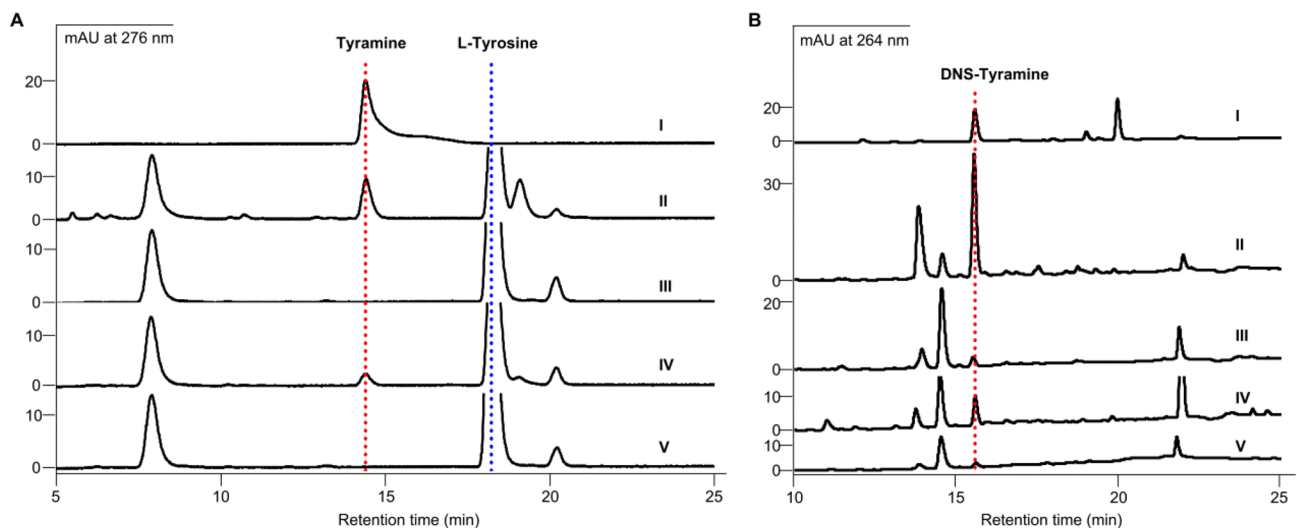


Fig. 5 Catalytic function characterization of LrTyDCs. **a** HPLC–DAD analyses of standard tyramine and the enzymatic reaction mixture of LrTyDCs. **b** HPLC–DAD analyses of the DNS derivatives of standard tyramine and the enzymatic reaction mixture of LrTyDCs. Panels I, the authentic tyramine and its DNS derivative; Panels II,

LrTyDC1-catalyzed reaction mixture and its derivatives; Panels III, boiled LrTyDC1 was used as catalyst; Panels IV, LrTyDC2-catalyzed reaction mixture and its derivatives; Panels V, boiled LrTyDC2 was used as catalyst. The vertical lines indicate that these peaks have identical retention time

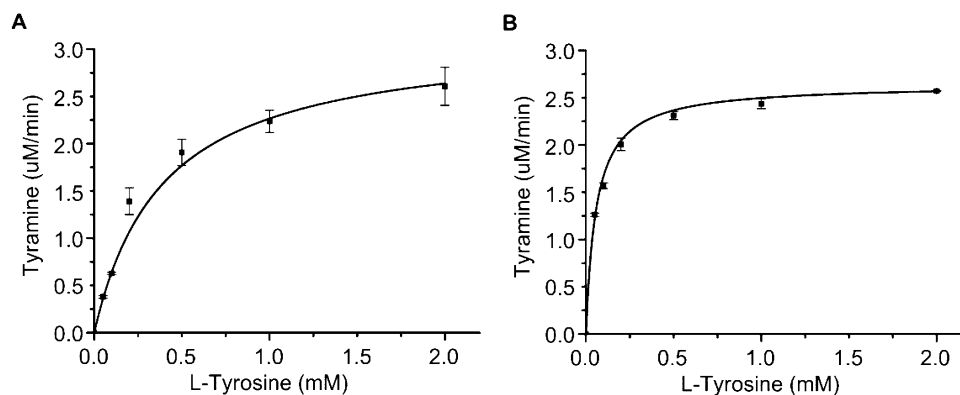


Fig. 6 The steady-state kinetic parameters for LrTyDC1- (**a**) and LrTyDC2- (**b**) catalyzed decarboxylation of L-tyrosine. The apparent kinetic parameters K_m and V_{max} for LrTyDC1-catalyzed decarboxylation reaction were 0.39 ± 0.14 mM and 3.15 ± 0.84 $\mu\text{M min}^{-1}$. The

K_m and V_{max} values for LrTyDC2-catalyzed decarboxylation reaction were 0.06 ± 0.007 mM and 2.64 ± 0.04 $\mu\text{M min}^{-1}$, respectively. Values represent the means of three replicates \pm SD

recognized as substrate of PsTyDC1 and PsTyDC2 (Facchini and De Luca 1994). TyDCs from Parsley (*Petroselinum crispum*) (Kawalleck et al. 1993) and *Eschscholtzia californica* (Marques and Brodelius 1988) could accept L-Tyr and occasionally L-DOPA, but not L-Trp or L-Phe. LaTyDC1, a TyDC from *L. aurea*, catalyzed the decarboxylation of L-Tyr and L-DOPA (Wang et al. 2019). For L-DOPA, LaTyDC1 exhibited a slight high K_m and a low V_{max} than those for L-Tyr (Wang et al. 2019). In this study, L-Tyr, L-Trp, L-Phe, and L-DOPA were used as potential substrates for LrTyDC-catalyzed decarboxylation reactions. The results showed that LrTyDCs catalyze decarboxylation of L-Tyr only (Fig. 5).

Transcriptional levels of LrTyDCs and GAL contents

Plant TyDCs have tissue expression specificity and associate with the accumulation of secondary metabolites in which L-Tyr is a precursor. For instance, *PsTyDC1* was highly expressed in poppy roots, while *PsTyDC2* was highly expressed in poppy roots and stems. Both of them were weakly expressed in leaves (Facchini and De Luca 1994). Herein both *LrTyDCs* were found to be widely expressed in *L. radiata* on the basis of qRT-PCR analyses (Fig. 7). The relative transcriptional levels of *LrTyDCs* in the roots are lower than those in other plant tissues (Fig. 7). Thus, all

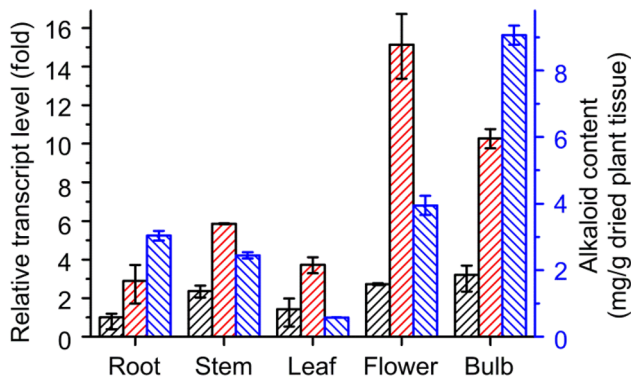


Fig. 7 The relationship of the transcript levels of *LrTyDCs* with the accumulation amount of GAL in *L. radiata*. The relative transcript levels of *LrTyDC1* (black column filled with black) and *LrTyDC2* (black column filled with red) in stems, leaves, flowers, and bulbs were normalized to that of *LrTyDC1* in roots. The contents of GAL were in blue column. Values represent the means of three biological replicates \pm SD

relative transcriptional levels were correlated with the lowest transcription level of *LrTyDC1* in roots (Fig. 7). *LrTyDC1* was shown to exhibit the highest transcript in bulbs, while it was the flowers in which *LrTyDC2* transcript was highest. *LrTyDC2* exhibited a slight lower transcriptional level in bulbs than that in flowers (Fig. 7). The relative transcripts of *LrTyDCs* in each plant tissue are directly proportionally correlated with the accumulation amount of GAL in the corresponding tissue of *L. radiata* according to the results reported previously (Fig. 7) (Li et al. 2019). Therefore, it was further confirmed that both *LrTyDCs* are involved in the decarboxylation of L-Tyr, the first biosynthetic step of GAL in *L. radiata*.

As an important biogenic amine, tyramine participates in a variety of physiological processes. For instance, tyramine is the essential component of the xylem cell wall (Borgolivier et al. 1987). It is the decisive factor in the overall defense system of plants such as parsley (Kawalleck et al. 1993) and *Arabidopsis* species (Trezza et al. 1993). When the cells were wounded, free and bound tyramine in the cell wall protected cells against viral infections (Negrel et al. 1993). Tyramine is a precursor of tyramine-derived natural products such as benzylisoquinoline alkaloids (Facchini et al. 2000, 2002) and the Amaryllidaceae alkaloids (Jin and Yao 2019; Jin 2009, 2013, 2016). The decarboxylation derivation of L-Tyr to generate tyramine is catalyzed by TyDCs, a group of enzymes between the primary and the secondary metabolisms. TyDCs are the pivotal and rate-limiting enzymes that connect primary metabolism and secondary metabolism, which determines the carbon flux of metabolic pathways. Plant TyDCs, a group II PLP-dependent decarboxylases, catalyze the decarboxylation of L-Tyr to generate tyramine, which is biologically important for diverting

essential primary metabolites into secondary metabolic pathways (Wang et al. 2020; Sandmeier et al. 1994). TyDCs are the committed enzymes and play an important role in regulating the first step of biosynthesis of secondary metabolites in plants (Guillet and De Luca 2005; Facchini and De Luca 1994). TyDCs are present in most, if not all, biological species (Kawalleck et al. 1993; Zahn et al. 1991; Eveleth et al. 1986; Morgan et al. 1986; Albert et al. 1987). In this work, two *TyDCs* were obtained from *L. radiata*, a GAL-producing plant, via transcriptome data analysis and molecular cloning. Heterologous expression of the aforementioned *LrTyDCs* in *E. coli* and following purification enable the in vitro biochemical characterization of recombinant *LrTyDCs*. Only L-Tyr was recognized by *LrTyDCs* to be decarboxylated to generate tyramine (Fig. 5). The transcript levels of *LrTyDCs* are correlated with the GAL contents in each specific tissue of *L. radiata* (Fig. 7), which implied their involvement in the biosynthesis of the Amaryllidaceae alkaloids. The reported works here will be helpful for biosynthetic investigations on the Amaryllidaceae alkaloids and for biological investigations on physiological processes.

Author contribution statement YL conceived and designed the experiments. JH, WL, and ZL performed the experiments. YL, JH, WL, and GZ analyzed the data and wrote the manuscript. All authors have read and approved the manuscript in its final form.

Supplementary Information The online version contains supplementary material available at <https://doi.org/10.1007/s11738-021-03258-6>.

Acknowledgements This work was supported in part by the 21172216 project from National Natural Science Foundation of China, the Biological Resources Programme, Chinese Academy of Sciences (KFJ-BRP-008), and the Applied and Basic Research Program of Sichuan Province (2015JY0058).

References

- Albert VR, Allen JM, Joh TH (1987) A single gene codes for aromatic L-amino acid decarboxylase in both neuronal and non-neuronal tissues. *J Biol Chem* 262:9404–9411
- Barton DHR, Kirby GW, Taylor JB, Thomas GM (1963) Phenol oxidation and biosynthesis. Part VI. The biogenesis of Amaryllidaceae alkaloids. *J Chem Soc* 1963:4545–4558
- Berkov S, Georgieva L, Kondakova V, Atanassov A, Viladomat F, Bastida J, Codina C (2009) Plant sources of galanthamine: phytochemical and biotechnological aspects. *Biotechnol Biotech Equip* 23:1170–1176
- Borgolivier SA, Tarlinton D, Brown KD (1987) Defective regulation of the phenylalanine biosynthetic operon in mutants of the phenylalanine-transfer RNA-synthetase operon. *J Bacteriol* 169:1949–1953
- Christenson JG, Dairman W, Udenfriend S (1972) On the identity of DOPA decarboxylase and 5-hydroxytryptophan decarboxylase. *Proc Nat Acad Sci USA* 69:343–347

- Desgagné-Penix I (2020) Biosynthesis of alkaloids in Amaryllidaceae plants: a review. *Phytochem Rev*. <https://doi.org/10.1007/s11101-020-09678-5>
- Eveleth DD, Gietz RD, Spencer CA, Nargang FE, Hodgetts RB, Marsh JL (1986) Sequence and structure of the dopa decarboxylase gene of *Drosophila*: evidence for novel RNA splicing variants. *EMBO J* 6:2663–2672
- Facchini PJ, De Luca V (1994) Differential and tissue-specific expression of a gene family for tyrosine/dopa decarboxylase in opium poppy. *J Biol Chem* 269:26684–26690
- Facchini PJ, De Luca V (1995) Expression in *Escherichia coli* and partial characterization of two tyrosine/dopa decarboxylases from opium poppy. *Phytochemistry* 38:1119–1126
- Facchini PJ, Huber-Allanach KL, Tari LW (2000) Plant aromatic L-amino acid decarboxylases: evolution, biochemistry, regulation, and metabolic engineering applications. *Phytochemistry* 54:121–138
- Facchini PJ, Hagel J, Zulak KG (2002) Hydroxycinnamic acid amide metabolism: physiology and biochemistry. *Can J Bot* 80:577–589
- Guillet G, De Luca V (2005) Wound-inducible biosynthesis of phytoalexin hydroxycinnamic acid amides of tyramine in tryptophan and tyrosine decarboxylase transgenic tobacco lines. *Plant Physiol* 137:692–699
- György Z, Jaakola L, Neubauer P, Hohtola A (2009) Isolation and genotype-dependent, organ-specific expression analysis of a *Rhodiola rosea* cDNA encoding tyrosine decarboxylase. *J Plant Physiol* 166:1581–1586
- Jin Z (2009) Amaryllidaceae and *Sceletium* alkaloids. *Nat Prod Rep* 26:363–381
- Jin Z (2013) Amaryllidaceae and *Sceletium* alkaloids. *Nat Prod Rep* 30:849–868
- Jin Z (2016) Amaryllidaceae and *Sceletium* alkaloids. *Nat Prod Rep* 33:1318–1343
- Jin Z, Yao G (2019) Amaryllidaceae and scelletium alkaloids. *Nat Prod Rep* 36:1462–1488
- Kawalleck P, Keller H, Hahlbrock K, Scheel D, Somssich IE (1993) A pathogen-responsive gene of parsley encodes tyrosine decarboxylase. *J Biol Chem* 268:2189–2194
- Kilgore MB, Kutchan TM (2016) The Amaryllidaceae alkaloids: biosynthesis and methods for enzyme discovery. *Phytochem Rev* 15:317–337
- Kilgore MB, Augustin MM, Starks CM, O'Neil-Johnson M, May GD, Crow JA, Kutchan TM (2014) Cloning and characterization of a norbelladine 4'-O-methyltransferase involved in the biosynthesis of the Alzheimer's drug galanthamine in *Narcissus sp aff pseudonarcissus*. *PLoS ONE* 9:e103223
- Lehmann T, Pollmann S (2009) Gene expression and characterization of a stress-induced tyrosine decarboxylase from *Arabidopsis thaliana*. *FEBS Lett* 583:1895–1900
- Li W, Yang Y, Qiao C, Zhang G, Luo Y (2018) Functional characterization of phenylalanine ammonia-lyase- and cinnamate 4-hydroxylase-encoding genes from *Lycoris radiata*, a galanthamine-producing plant. *Int J Biol Macro* 117:1264–1279
- Li W, Qiao C, Pang J, Zhang G, Luo Y (2019) The versatile O-methyltransferase LrOMT catalyzes multiple O-methylation reactions in amaryllidaceae alkaloids biosynthesis. *Int J Biol Macro* 141:680–692
- Maldonado-Mendoza IE, López-Meyer M, Galef JG, Burnett R, Nessler CL (1996) Molecular analysis of a new member of the opium poppy tyrosine/3,4-dihydroxyphenylalanine decarboxylase gene family. *Plant Physiol* 110:43–49
- Marco L, Carreiras MC (2006) Galanthamine, a natural product for the treatment of Alzheimer's disease. *Recent Pat CNS Drug Discov* 1:105–111
- Marco-Contelles J, Carreiras MC, Rodríguez C, Villarroya M, García AG (2006) Synthesis and pharmacology of galantamine. *Chem Rev* 106:116–133
- Marques IA, Brodelius PE (1988) Elicitor-induced L-tyrosine decarboxylase from plant cell suspension cultures: I. Induction and purification. *Plant Physiol* 88:46–51
- Morgan BA, Johnson WA, Hirsh J (1986) Regulated splicing produces different forms of dopa decarboxylase in the central nervous system and hypoderm of *Drosophila melanogaster*. *EMBO J* 6:3335–3342
- Negrel J, Javelle F (2001) L-Tyrosine beta-naphthylamine is a potent competitive inhibitor of tyramine N-(hydroxycinnamoyl)transferase in vitro. *Phytochemistry* 56:523–527
- Negrel J, Javelle F, Paynot M (1993) Biochemical basis of resistance of tobacco callus tissue cultures to hydroxyphenylethylamines. *Plant Physiol* 103:329–334
- Noé W, Mollenschott C, Berlin J (1984) Tryptophan decarboxylase from *Catharanthus roseus* cell suspension cultures: purification, molecular and kinetic data of the homogenous protein. *Plant Mol Biol* 3:281–288
- Park S, Lee K, Kim YS, Chi Y, Shin JS, Back K (2012) Induced tyramine overproduction in transgenic rice plants expressing a rice tyrosine decarboxylase under the control of methanol-inducible rice tryptophan decarboxylase promoter. *Bioproc Biosyst Eng* 35:205–210
- Sandmeier E, Hale TI, Christen P (1994) Multiple evolutionary origin of pyridoxal-5'-phosphate-dependent amino acid decarboxylases. *Eur J Biochem* 221:997–1002
- Singh A, Desgagné-Penix I (2017) Transcriptome and metabolome profiling of *Narcissus pseudonarcissus* 'King Alfred' reveal components of Amaryllidaceae alkaloid metabolism. *Sci Rep* 7:17356
- Singh A, Massicotte MA, Garand A, Tousignant L, Ouellette V, Bérubé G, Desgagné-Penix I (2018) Cloning and characterization of norbelladine synthase catalyzing the first committed reaction in Amaryllidaceae alkaloid biosynthesis. *BMC Plant Biol* 18:338
- Son M, Kim A, Lee J, Park C, Heo J, Lee H, Lee S (2010) Ethanol extract of *Lycoris radiata* induces cell death in B16F10 melanoma via p38-mediated AP-1 activation. *Oncol Rep* 24:473–478
- Sun B, Wang P, Wang R, Li Y, Xu S (2018) Molecular cloning and characterization of a *metalpara*-O-methyltransferase from *Lycoris aurea*. *Int J Mol Sci* 19:1911
- Takos AM, Rook F (2013) Towards a molecular understanding of the biosynthesis of Amaryllidaceae alkaloids in support of their expanding medical use. *Int J Mol Sci* 14:11713–11741
- Torrens-Spence MP, Lazear M, von Guggenberg R, Ding H, Li J (2014) Investigation of a substrate-specifying residue with *Papaver somniferum* and *Catharanthus roseus* aromatic amino acid decarboxylases. *Phytochemistry* 106:37–73
- Trezzini GF, Horrichs A, Somssich IE (1993) Isolation of putative defense-related genes from *Arabidopsis thaliana* and expression in fungal elicitor-treated cells. *Plant Mol Biol* 21:385–390
- Wang R, Han X, Xu S, Xia B, Jiang Y, Xue Y, Wang R (2019) Cloning and characterization of a tyrosine decarboxylase involved in the biosynthesis of galanthamine in *Lycoris aurea*. *Peer J* 7:6729
- Wang H, Yu J, Satoh Y, Nakagawa Y, Tanaka R, Kato K, Yao M (2020) Crystal structures clarify cofactor binding of plant tyrosine decarboxylase. *Biochem Biophys Res Commun* 523:500–505
- Wu D, Huang H, Cai C, Sha R (2018) Study on the optimization of derivative conditions of biomidan sulfonyl chloride. *Food Ferment Sci Technol* 54:45–49
- Yang R, Zeng Q (2005) Cloning, sequencing and homologous analysis of tyrosine decarboxylase gene from *Aristolochia contorta* Bge. *J Guangzhou Univ Trad Chin Med* 22:152–156
- Zahnow A, Yi H, McBride OW, Joseph DR (1991) Cloning of the cDNA encoding human histidine decarboxylase from an

- erythroleukemia cell line and mapping of the gene locus to chromosome 15. *DNA Seq* 1:395–400
- Zhang J, Ma L, Yu H, Zhang H, Wang H, Qin Y, Shi G, Wang Y (2011) A tyrosine decarboxylase catalyzes the initial reaction of the salidroside biosynthesis pathway in *Rhodiola sachalinensis*. *Plant Cell Rep* 30:1443–1453
- Zhang L, Yu Q, Zhang Z, Liu Y, Wang Y, Xin Z (2018) Determination of eight biogenic amines in fermented drinks by reversed-phase high-performance liquid chromatography with precolumn derivatization. *Chin J Health Lab Technol* 28:2057–2059
- Zhou S, Yu B, Luo Q, Hu J, Bi D (2007) Karyotypes of six populations of *Lycoris radiata* and discovery of the tetraploid. *Acta Phytotaxon Sin* 45:513–522

Publisher's Note Springer Nature remains neutral with regard to jurisdictional claims in published maps and institutional affiliations.